Measurements of displacement and trapping force on micron-sized particles in optical tweezers system

GUO Honglian (郭红莲)[1], YAO Xincheng (姚新程)[1], LI Zhaolin (李兆霖)[1], CHENG Bingying (程丙英)[1], HAN Xuehai (韩学海)[2] & ZHANG Daozhong (张道中)[1]

1. Optical Physics Laboratory, Institute of Physics and Center for Condensed Matter Physics, Chinese Academy of Sciences, Beijing 100080, China;
2. State Key Laboratory of Biomacromolecules, Institute of Biophysics, Chinese Academy of Sciences, Beijing 100101, China

Correspondence should be addressed to Guo Honglian (email: redlotus@aphy.iphy.ac.cn)

Received September 24, 2001

Abstract A high-stability optical tweezers equipped with a high-precision measurement system of displacement and force is set up. The results show that this combination can be used to carry out quantitative measurements of small displacements and forces for micron-sized spheres. The precision of measurements has reached nanometers and piconewtons, respectively.

Keywords: optical tweezers, displacement, force.

Optical tweezers is a three-dimensional gradient optical trap. The tapping force comes from momentum exchange between photons and trapped particles. Because it allows non-contact and non-intrusive manipulation of living objects and its piconewton force (10^{-12}N) is well suitable for the study of dynamic properties of cells, sub-cells and macromolecules, optical tweezers have been extensively applied to biological researches and show strong vitality[1—5]. Moreover, in the field of physics it can be used for the study of Brownian motion of micron-sized bead, interactions between like-charge spheres, the motion of micro-spheres under a magnetic field, and so on[6—8]. Due to its broad prospects the requirement for the measurement precision of displacement and force is getting higher. Presently, quantitative measurements of nanometer displacements and sub-piconewton forces have received much attention. For example, the tiny displacement and force resulted from the relative sliding of actin and myosin filaments during muscle contraction have been measured. In this paper, we describe the methods of displacement and force measurements on 1-μm-diameter polystyrene bead. The results show that the precision of displacement and force is at nanometers and sub-piconewtons level, respectively.

1 The theory and structure of optical tweezers

The principle of optical tweezers may be briefly described as shown in fig. 1. When a tight focused laser beam passes through a dielectric sphere with a refractive index greater than the surrounding medium, the propagation direction of the incident beam changes, i.e. the momentum of

photons is no longer the same as before. By the rule of momentum conservation the reaction may be exerted on the spheres. According to the Newton's Second Law the change rate of the momentum corresponds to the interaction force.

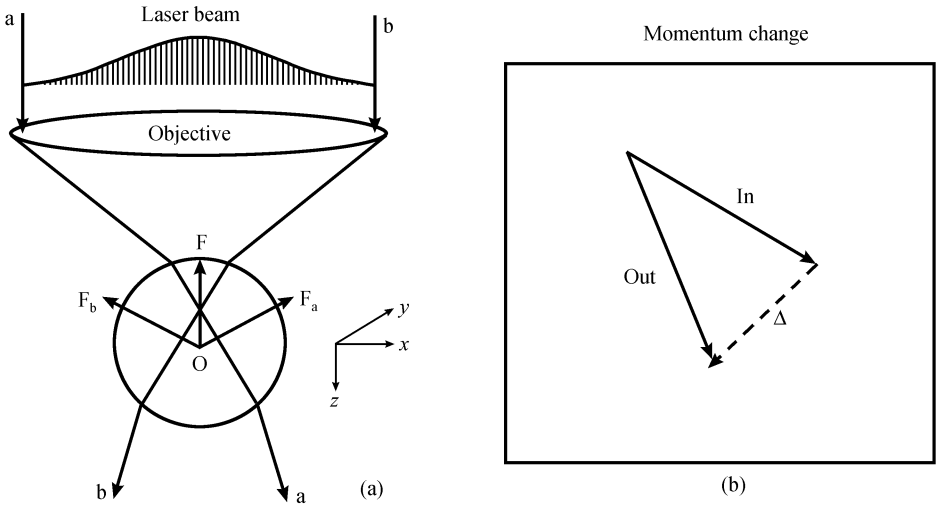

Fig. 1. (a)A ray-optic picture of the optical gradient force. The two representative rays (a, b) of a parallel beam pass through a high numerical aperture (NA≥1) microscope objective. The rays are bent by refraction. (b) Schematic diagram of momentum change, showing a vector diagram of momentum change for photons in ray a.

Schematic diagram of the optical trap is shown in fig. 2. The solid lines represent the path of the laser, while the dashed lines are the illuminating light from a tungsten lamp. Lenses L1 and L2 consist of a beam expander, by which the light of beam is adjusted to fill the back aperture of the microscope objective. It results in the increase of the trapping efficiency, as well as the trapping force. Lens L3 and Tube lens are confocal. The specimen is illuminated by a focused beam, which is created by the Tungsten lamp and lenses C1 and C2. Image of the specimen is projected on the front surface of the CCD (charge coupled device) camera.

2 Measurement of displacement

In the optical tweezers system, polystyrene bead is usually used as a "handle" by binding to the biological object so that the movement of the biological object can be obtained by measuring that of the bead. One of the methods of measuring the movement of the bead is the intensity weighted centroid of bead image. Since the movement of intensity weighted centroid of the bead image is corresponded to that of the bead itself, the displacement of the bead can be calculated by measuring the movement of its intensity weighted centroid which is defined as the average position of pixels containing the bead image weighted by the pixel intensity [9,10]. The coordinates of the centroid (x, y) are computed as follows:

$$x = \sum_{i=1}^{m}\sum_{j=1}^{n} i \cdot g(i, j) / I_{\text{sum}}, \quad y = \sum_{i=1}^{m}\sum_{j=1}^{n} j \cdot g(i, j) / I_{\text{sum}}, \quad I_{\text{sum}} = \sum_{i=1}^{m}\sum_{j=1}^{n} g(i, j), \tag{1}$$

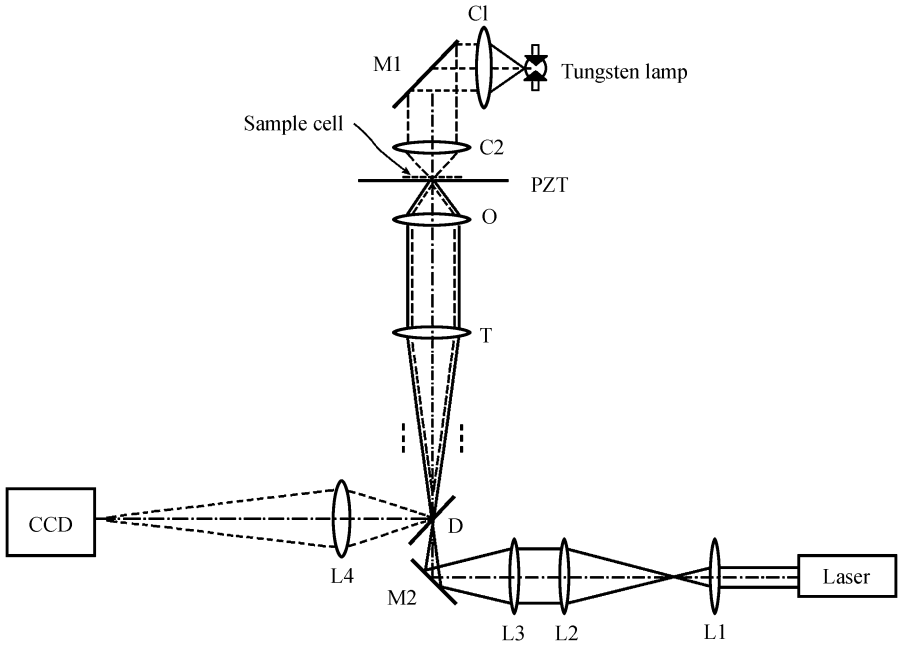

Fig. 2. Schematic diagram of the optical tweezers system. L1 and L2, Lenses for beam expanding; M1 and M2, mirrors for beam steering; O, microscopy objective (HCXAPO 100×/1.30); C1 and C2, lenses for illumination light condensing; D, dicroic filter; L4, auxiliary lens for imaging; PZT, piezo-electric-transducers used for micro-operation of sample cell and force calibration.

where (x, y) is taken as the position of bead image; m, n are the numbers of pixels included in the bead image in horizontal and vertical directions, respectively; (i, j) is coordinates of pixel; $g(i, j)$ is its corresponding intensity.

In order to know the error of this method, the simulation calculation was carried out with different ratios of bead radius to pixel size. In the calculation, the intensity of the bead image is assumed to be homogeneous. Fig. 3(a) shows the schematic diagram of the bead image on the surface of CCD camera and fig. 3(b) shows the relationship between the error and the movement of the bead with different ratios of r to a. From fig. 3(b) it can be seen that the error is very small when the ratio of r to a is large enough.

In our experiments, the scientific microscope (Leica DMIRB) and oil-immersion objective were used for observing the micro-object and focusing the laser beam. The sample cell which consisted of two coverslips was put on the stage of the microscope and its depth was about 100 μm. In the force calibration the polystyrene bead suspended in water was chosen as a target object and could be focused with different depths by adjusting the axial position of the objective, whereas in the measurements of the system stability and the performance of PZT, the bead was attached to the bottom of the sample cell. The bead was magnified 100- and 6-fold by the objective and the auxiliary lens L4, respectively, then projected on the front surface of the CCD camera (Cohu 4912). The magnification was calibrated against the 10 μm ruling micrometer. The pixel

size of CCD was 8.4 μm × 8.9 μm, so the number of pixels included in the bead image was about 3782. The image acquired by 8-bit mono-video image acquisition card was recorded in the computer. According to the frame-by-frame difference of the bead image positions, the displacement of the bead can be obtained.

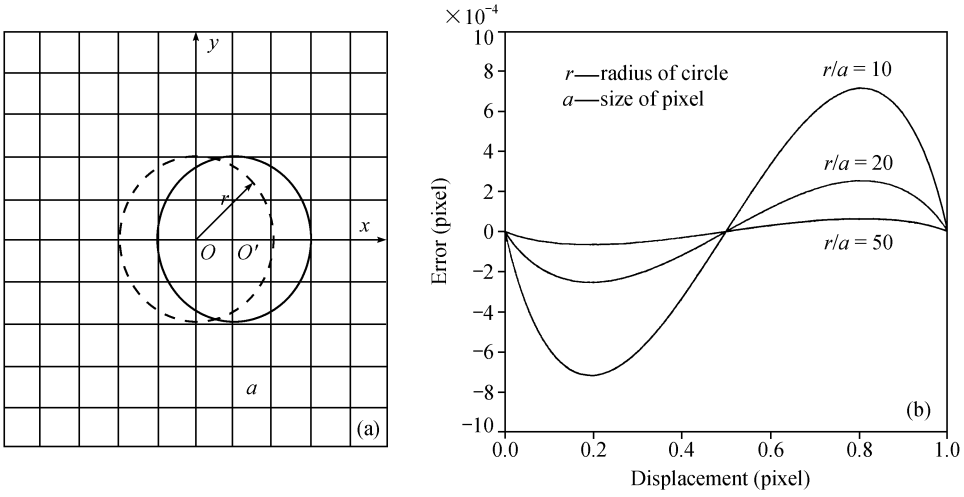

Fig. 3. (a) Schematic diagram of bead image; a rectangular sub-region represents a pixel; *r*, radius of the bead image; *a*, the size of pixel. The dashed circle is the image of a bead at its initial position *O* and the solid one is that of the shifted bead. *OO′* is the displacement of the bead. (b) The relationship between displacement and the error with different ratios of *r* to *a*.

In the experiments, the factors which influenced the precision of the displacement measurements were various such as the stability of the table, the image quality and the bead magnification. To know about the displacement resolution of the system, we tracked the position of the bead attached to the bottom of the coverslip with magnification of 600 times (fig. 4). The time sequence frame (time interval 40 ms) was recorded. The positions of the bead image can be calculated by eq. (1). Fig. 5 shows the *x* coordinate of a bead position during a total acquisition period of 3.2 s. The same is true to the *y* coordinate. The standard deviation of the positions computed in this way is 0.7 nm, which suggests that the displacement resolution limit of the system is nanometer-level.

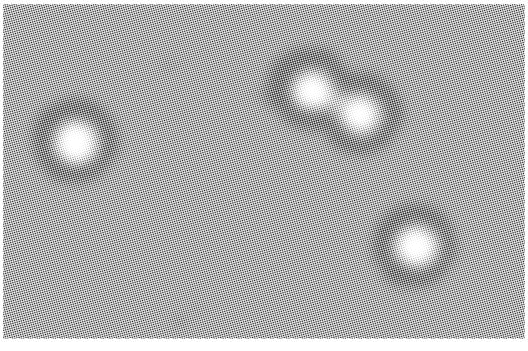

Fig. 4. The picture of the 1-μm polystyrene bead magnified, × 600.

As an application of this method, we examined the movement of one-dimensional piezo-electric sub-stage driven by the triangular wave input just by measuring the movement of bead attached to the bottom of coverslip which is carried by this stage. Fig. 6 shows its movement track. It is seen that the total movement range

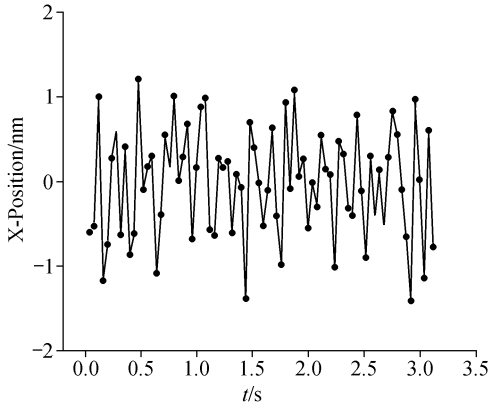

Fig. 5. Immobilized bead track in x axis. • represents the x coordinate with a sampling interval of 40 ms.

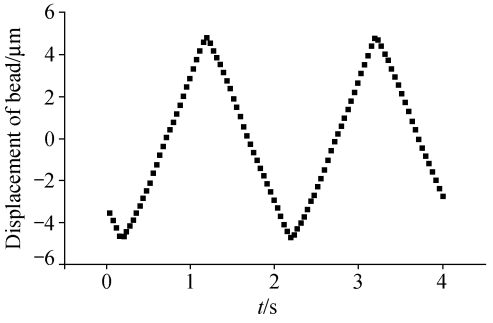

Fig. 6. Movement of piezo-electric transducer.

of the bead, i.e. the piezo-electric transducer, is 9.6 μm and the relationship between the position of transducer and voltage input is linear.

To further test its performance, we monitored the vibration of PZT in the direction perpendicular to its movement. The measurement method was the same as that mentioned above. Fig. 7 shows the relationship between the vibration (y axis) and the displacement (x axis) of PZT. Two lines represent a periodic motion. The maximum deviation in the y direction is 23 nm. So the ratio of maximal vibration and displacement is 0.023/9.6 = 0.24%.

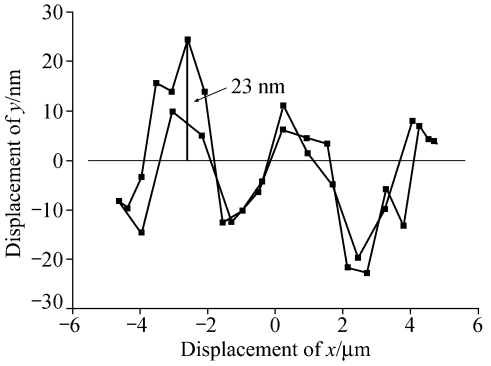

Fig. 7. Vibration of a PZT in the direction perpendicular to its movement.

3 Force calibration

When an external force is applied to a bead held by an optical trap, the bead is displaced from the center of the trap. At this moment, the trap exerts a force, which is equal and opposite to the external force to the bead to balance the bead. The relation between the trapping force F and laser power p can be written as [11−15]

$$F=Qn_1P/c, \tag{2}$$

where Q is a dimensionless efficiency parameter, n_1 is the refractive index of the surrounding medium, and c is the speed of light in free space. Based on eq. (2) the trapping force is directly proportional to Q in certain surrounding medium and laser power. Calculation of the trapping force was performed with a ray-optics (RO) model[11, 12]. Fig. 8 shows the dependence of Q on the displacement of bead from the center of the trap. It is seen that when the displacement of the bead is less than its radius, Q is approximately proportional to the bead displacement. So the force-displacement relationship is close to a line in a certain range of displacement, which can be

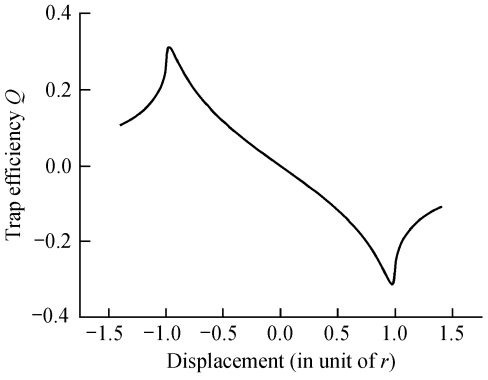

Fig. 8. *Q versus* displacement of bead. The zero of *x* coordinate represents the optical trap center. *r* is the radius of bead.

described as:

$$F = kx, \tag{3}$$

where x is the bead displacement, k is the stiffness of the trap. Therefore, once the displacement of the bead is obtained, the trapping force can be deduced.

In order to know the trapping force more precisely, a fluid dynamics method was adopted to calibrate the force. The fluid flows past the trapped bead, due to the viscous force exerted by the fluid flow, the bead is displaced from the center of the trap. When the viscous force equals to the trapping force, the bead stays in a stable position. Thus, the force can be calculated from Stokes' law [5]: $F=6\pi\eta r\nu$, where v is the velocity of fluid, η is the viscosity of fluid and r is the radius of bead. In our experiments, the fluid flow was produced by moving one-dimensional piezo-electric driven sub-stage on which the sample cell was placed. The corresponding experimental setup is schematically given in fig. 9.

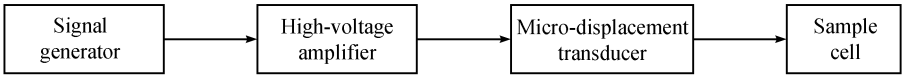

Fig. 9. Block diagram of force calibration.

Under the condition of the laser (He-Ne) power 5 mW (measured before the objective), we measured displacements of bead from the center of the trap under different viscous force applied to 1-μm-diameter polystyrene bead trapped by the optical tweezers. Fig. 10 shows the force-displacement relationship for the optical tweezers. From eq. (3), it is known that the slope of linear fit is the trap stiffness k = 0.005 pN/nm. When the trap stiffness is known, the force on the bead can be easily calculated from the displacement of bead multiplied by the trap stiffness.

In conclusion, high-precision displacement and force measurements system was set up and measurements were carried out on 1-μm-diameter polystyrene. Results show that the precision of displacement and force is at nanometer and sub-piconewton scale, respectively. With this system, we quantitatively measured the transverse vibration of PZT. This may be a new way for testing the performance of PZT. Our experiments indicate that the system described above may be used for precise measurements of small displacement and force in both biological and

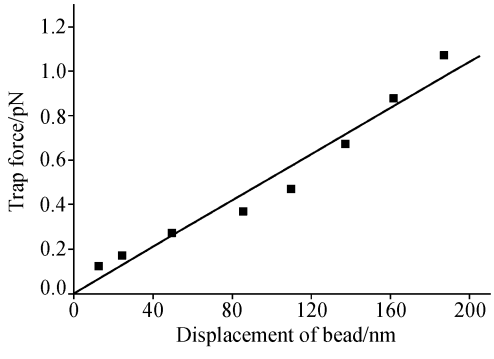

Fig. 10. Calibration of the trap stiffness.

physical fields.

Acknowledgements This work was supported by the National Natural Science Foundation of China (Grant No. 1989380).

References

1. Ashkin, A., Dziedic, J. M., Bjorkholm, J. E. et al., Observation of a single-beam gradient force optical trap for dielectric particles, Opt. Lett., 1986, 11(5): 288—290.
2. Ashkin, A., Dziedic, J. M., Optical trapping and manipulation of viruses and bacteria, Science, 1987, 235: 1517—1520.
3. Ashkin, A., Dziedic, J. M., Yamane, T., Optical trapping and manipulation of single cells using infrared laser beams, Nature, 1987, 330(24): 769—771.
4. Finer, J. T., Simmons, R. M., Spudich, J. A., Single myosin molecule mechanics: Piconewton forces and nanometer steps, Nature, 1994, 368: 113—119.
5. Svoboda, K., Block, S. M., Biological application of optical forces, Annu. Rev. Biophys. Biomol. Struct., 1994, 23: 247—285.
6. Simmons, R. M., Finer, J. T., Steven, C. et al., Quantitative measurement of force and displacement using an optical trap, Biophysics Journal, 1996, 70: 1813—1822.
7. Bowen, W. R., Sharif, A. O., Long-range electrostatic attraction between like-charge spheres in a charged pore, Nature, 1998, 393: 663—665.
8. Wen Weijia, Zhang Lingyun, Sheng Ping, Planar magnetic colloidal crystals, Phys. Rev. Lett., 2000, 85(25): 5464—5469.
9. Gelles, J., Bruce, J., Michael, P. S., Tacking Kinesin-driven movements with nanometer-scale precision, Nature, 1988, 331: 450—453.
10. Dai Jianwu, Michael, P. S., Cell membrane mechanics, Methords in Cell Biology, 1998, 55: 157—170.
11. Ashkin, A., Forces of a single-beam gradient laser trap on a dielectric sphere in the ray optics regime, Biophys. J., 1992, 61: 569—582.
12. Yao Xincheng, Li Zhaolin, Cheng Bingying et al., Increasing transverse stability of optical tweezers by using dual-gaussian beam profile, Chin. Phys., 2000, 9(1): 65—68.
13. Yao, X. C., Li, Z. L., Cheng, B. Y. et al., Analysis and calculation of the optical force on a double-layer dielectric sphere, 2000, 20(10): 1305—1310.
14. Yao, X. C., Li, Z. L., Guo, H. L. et al., Effects of spherical aberration on optical trapping forces for rayleigh particles, Chinese Physics Letter, 2001, 18(3): 432—434.
15. Yao, X. C., Li, Z. L., Guo, H. L. et al., Effect of spherical aberration introduction by water solution on trapping force, Chinese Physics, 2000, 9(11): 824—826.